

# Low Cycle Fatigue Failure of a Sitka Spruce Tree in Hurricane Winds

By Warren B. Leigh

**Abstract.** Pine plantations are prone to stem breakage due to high cyclic stress levels associated with hurricane force winds. Stress analytical and finite element simulation models were constructed of a representative profile of a (Sitka) *Picea sitchensis* tree. The profile surface stress ( $S$ ) was determined due to the combined load of tree self-weight and hurricane wind speed. The results were complemented by reference to two other studies by other researchers that investigated the impact of fatigue cycles on failure ( $N$ ) of pine wood and tree sway cycles to present a stem fatigue life prediction. The position of maximum surface profile stress and trunk fracture initiation location was ascertained from a non-uniform stress response. No stress uniformity along the trunk profile was observed for any wind-load case examined. The analytical model and finite element analysis of the *P. sitchensis* tree trunk profile revealed a statically adequate strength reserve factor of 1.4, which suggested another mode of failure was responsible. Fatigue life failure prediction was examined under cyclic and same-stress amplitude related to the hurricane wind speed of  $33 \text{ m s}^{-1}$ . Predicted trunk fracture occurred in 2.6 hours, which dramatically reduced to two minutes with an increase in wind speed of only  $1 \text{ m s}^{-1}$ . The calculated exposure time was similar to that recorded during Hurricane Hugo's transit in 1989. The time-to-failure prediction obtained by the method of analysis provided in this study seemed plausible, and that the profile associated with the *P. sitchensis* tree would suffer trunk breakage by low cycle fatigue failure.

**Key Words.** Failure; Fatigue; Finite Element Analysis; Hurricane; *Picea sitchensis*; Sitka Spruce; Stress; Wind; Wind Load.

Mechanical parts may fail due to accumulating damage from fluctuating stresses. These stresses are normally below the ultimate and yield strength of the material. Failure by cyclic loading is known as fatigue failure. Some materials, such as steel, show an infinite stress life below a certain stress level known as the endurance limit. The ratio of the endurance limit stress to the ultimate stress of the material defines the fatigue ratio, which ranges from 0.25 to 0.6 for metals. Bao et al. (1996) reported that for all the wood materials tested, an endurance limit was achieved when stress levels were at 0.3 of the ultimate strength of the wood. Fatigue failure of their specimens began around 0.4.

As wind speeds increase towards recognized hurricane levels of Beaufort scale 12 ( $33 \text{ m s}^{-1}$ ), tree damage is observed as a successive and incremental process initiating with defoliation, at  $17 \text{ m s}^{-1}$ , to trunk breakage, at over  $33 \text{ m s}^{-1}$  (Cullen 2002; James and Haritos 2006). Observation of the damage caused by Hurricane Hugo in 1989 revealed that no trunk breakage occurred below wind gust

speeds of  $33 \text{ m s}^{-1}$ . The probability of damage to a tree increased with gust intensity (Francis and Gillespie 1993). The uniform stress distribution axiom in tree profiles rest on the supposition that a tree profile adapts a shape in response to time-averaged load conditions along its length. This profile tapering is purported to equalize the probability of material failure along the profile length as the stress remains constant (Larson 1964; Wilson and Archer 1979; Mattheck 1991; Morgan and Cannell 1993). However, mathematical tree models by Gaffrey (1999) and a tree-pulling field test by Clair (2003) reported non-uniform surface stress distributions decreasing from tree profile top to its base.

In this investigation, where finite element analysis (FEA) confirmed for all the wind speed load cases applied to the *Picea sitchensis* tree profile model, a non-uniform stress distribution of higher stress magnitude occurred at the top of the tree profile than at its base. Similar results were found on simulated profile models of nine different species of trees analyzed by the author on a separate study (Leigh

2012), using both analytical and finite element stress analysis. No statistical tree survey was made due to resource and budget confines. The mathematical model was used to determine the tree's profile surface stress and essentially emulated the methods described by other researchers (Gaffrey 1999; Niklas and Molina-Freaner 1999). Tree growth stress was not included in the mathematical model.

Biological and mechanical constraints on trees influence their growth, but wood has a structural limit, and similar to metal, it is susceptible to failure by static or fatigue loading (Bao et al. 1996). Static strength of a tree may be reflected by the magnitude of wind load the trunk can sustain before breakage ensues. Published data of ultimate strength values for fresh, green-condition Scots pine was  $46 \text{ N mm}^{-2}$  (Petty and Swain 1985). However, to allow for statistical variation and defects a factor of 70% was applied, giving a final pine wood breaking stress of  $32 \text{ N mm}^{-2}$  (Fons and Pong 1957). Strength data on *P. sitchensis* is similar and is published as an average of  $34 \text{ N mm}^{-2}$  (Moore 2011).

Structures often fail by fatigue under cyclic load events that are less than the static strength of the material (Niklas and Molina-Freaner 1999). Hurricanes impose high cyclic stress levels on trees, and the stress effects from lower wind-speed events, although transient, may accumulate. Relatively few cycles at high stress levels can result in structural failure by low cycle fatigue (LCF) (Gong and Smith 2000). Alternatively, lower but repeated stress levels may result in failure by high cycle fatigue. Fatigue of wood is controlled by number of cycles to failure ( $N$ ) and load exposure time. The conventional fatigue characterization is the number of cycles to failure ( $N$ ) at a particular stress level ( $S$ ), producing  $S-N$  curves (Clorius 2002). The fatigue of wood is generally species independent (Tsai and Ansell 1990), offering the opportunity to transpose the  $S-N$  curve to other species. The order of wood fatigue strength was similar on average endurance stress levels at 25% of a wood's MOR (Ratnasingam and Loras 2010). Stress levels and stress reversal produced the most fatigue damage (Bao and Gibson 1996).

Tree movement in the wind has been described by Coder (2000) as the sway frequency of the tree stem harmonizing with wind gust frequencies. Coder (2000) presents a table of natural sway frequencies in cycles per minute and for time to complete one cycle

of reversal, related to stems of different heights. The time-dependent cyclic effect plays a primary role in damage accumulation in the wood cells. This may be represented by a stress level ( $S$ ) equated to the number of cycles to failure, presenting a fatigue life.

Life determination of the number of cycles to fatigue failure ( $N$ ) was assessed using repeated load cycles of constant stress amplitude ( $S$ ) related to the conventionally known  $S-N$  curves specific for wood (Bao and Gibson 1996). Further processing with harmonic cyclic tree sway data time to tree stem failure was calculated expressed in log hours (hours) and log minutes for various wind-induced stress levels (Coder 2000).

## METHODS AND MATERIALS

### Low Cycle Fatigue Failure Derivation Methodology

A flowchart (Figure 1) is provided that describes all of the necessary steps that defined the process leading to the LCF failure analysis. Supportive explanations associated with each step in the flowchart follow.

### Site Location

The *P. sitchensis* tree (Figure 2) study was located in the Derbyshire region of Great Britain. Dimensional data of a suitable stem profile was obtained in early spring 2012. The tree stood in a small plantation (Lat. 53.38, Long. -1.716) at an elevation of 182.9 m, adjacent to a small but lively freshwater stream that feeds the Ladybower Reservoir.

### Field Data

Field data measurements were obtained from a selected non-meandering, approximately vertical *P. sitchensis* profile. The profile length is defined from root to the underside of crown, which has evolved due to the prevailing winds and is visually more profound. The selected leeward profile was photographed at 90 degrees to the prevailing wind. Representative coordinates were extracted and directly measured or visually assessed from photographic data to provide the form of the mathematical models developed in the analysis. The data included the crown height, width, profile height, tip, base diameter, and leaf volume fraction percentage that occupied the crown. The tree diameter was obtained from one cir-

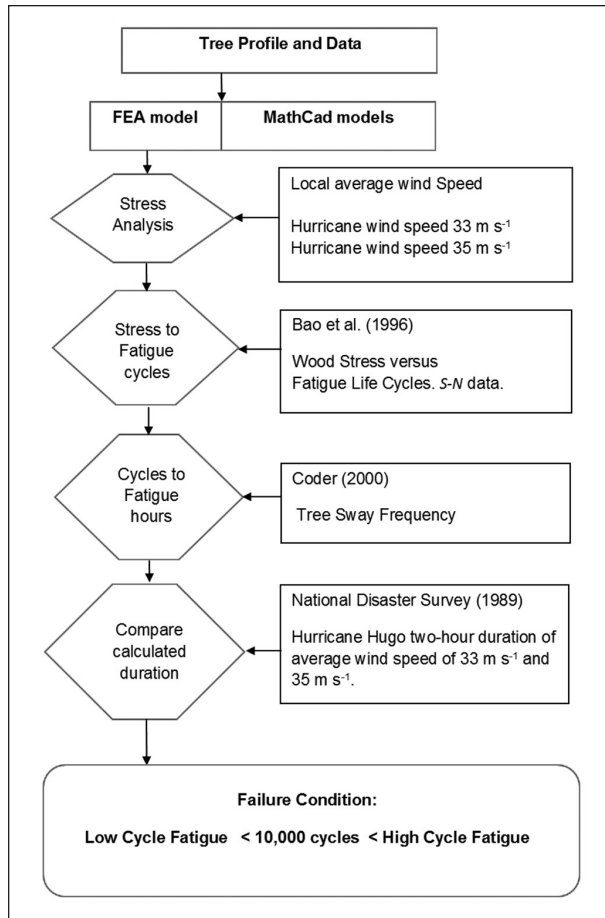


Figure 1. Flowchart for low cycle fatigue failure.

cumferential measurement at breast height (DBH), assumed 1500 mm above the tree base. The tree height measurement used trigonometric techniques (Figure 3) (Farmers Forest 2006). The tree dimensional values are listed in Table 1. The tree appeared to be in good health with no obviously decayed regions.

### Analytical Solutions and Supportive Data

An analytical, closed-formed solution was written in the commercially available mathematical software package (PTC MathCad®, PTC Inc., Needham, Massachusetts, U.S.) to evaluate the profile stresses. The applied load in the structure was due to the combined load of wind load and the tree's self-weight. The mathematical model represented the tree's unique profile as a solid cantilever fixed at its base. A point load expressing the wind force ( $F_c$ ) applied at the center of the crown produces a bending moment when combined with the lever arm and consequently a wind-induced

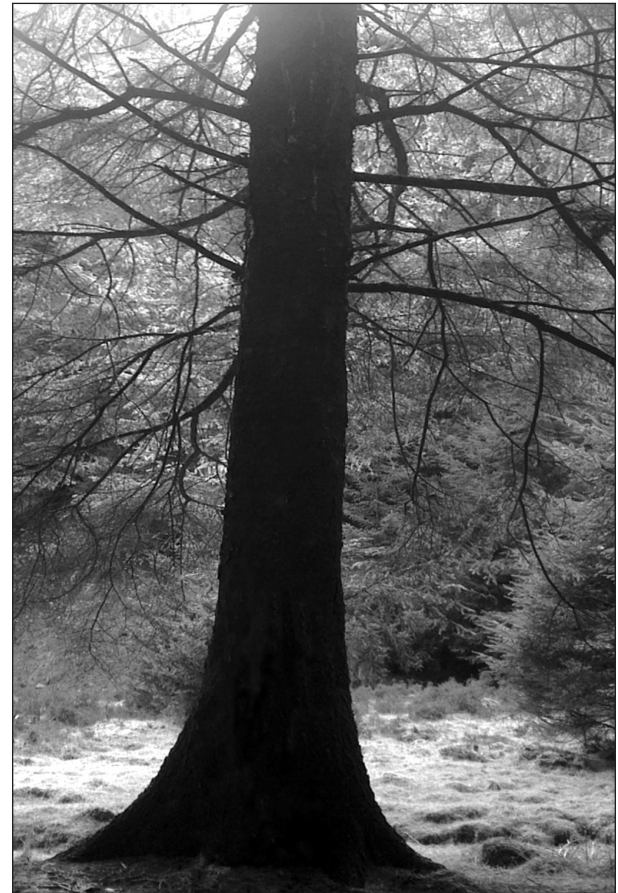


Figure 2. *Picea sitchensis*. Location: Snake Pass, 2012.

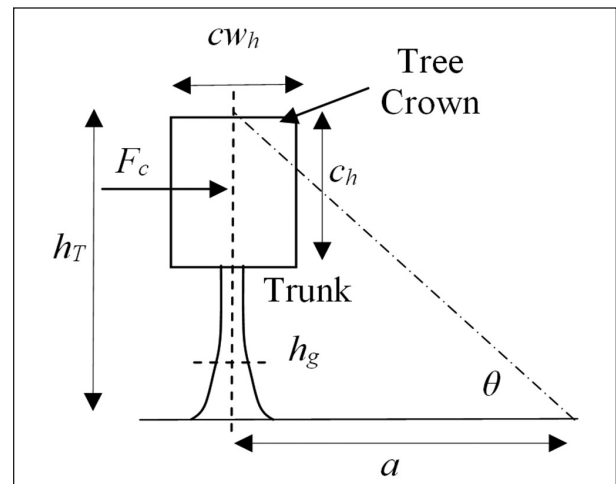


Figure 3. Idealized tree and dimensional parameters:

- $cw_h$  = Crown width (m)
- $F_c$  = Point wind force (N)
- $c_h$  = Crown height (m)
- $h_r$  = Ground to Crown top dimension (m)
- $h_g$  = Breast height (mm)
- $\theta$  = Trig angle subtended
- $a$  = Adjacent distance for trigonometric height

**Table 1. *Picea Sitchensis* dimensional measurements, properties, wind force, and moment data.**

Height (m)	Diameter (DBH) (mm)	Taper ratio	Crown height (m)	Crown width (m)	Profile tip height (mm)	Tip radius (mm)	Moment height (m)	Tree weight (kg)	Wind velocity (m s <sup>-1</sup> )	Leaf plumage (%)	Crown force (N)	Moment at (DBH) (N mm)
34.0	700.0	49.0	31.0	5.5	5600.0	181.0	17.0	6158.0	4.2	0.5	736	1.25E+07
									33.0	1.0	12390	2.11E+08

stress on the breast-height section. The distance from the section to the load application position gives the lever arm distance. The numerical solutions were made in a general purpose, finite element package (MSC Patran-Nastran, MSC Software Corporation, Newport Beach, California, U.S.) to examine the stress distribution. The breast-height section was chosen as a suitable location to check the FEA numerical model stress results against the classical analytical (MathCad model) solution.

A variety of wind-load cases were examined in this study, including that of the local yearly average wind speed and the hurricane wind speed of 33 m s<sup>-1</sup> (Cullen 2002; James and Haritos 2006).

The analytical model developed for this study used the same wind-load drag formula as referenced by Niklas and Molina-Freaner (1999) and Cullen (2005). The trunk profile structure was treated as an elastic perpendicular cantilever beam rigidly fixed at its base. The y-direction of the Cartesian coordinate system was in-line with the vertical axis of the cantilever.

The stress analysis was made of the assumed circular section (Timoshenko 1930) of the trunk profile that related to DBH at 1500 mm above local ground level. No allowance was made to the degree of fixity influence by the tree root and soil conditions in either of the simulations. The density of air ( $\rho_a$ , kg m<sup>-3</sup>) was assumed to be constant at 1.22 kg m<sup>-3</sup>. The wind force ( $F_c$ ) (Newtons) was applied as a horizontal constant force acting at the center of pressure on the crown for all the wind-load cases and used the coefficient of drag Equation 1 (Cullen 2005).

$$[1] \quad F_c = 0.5 \times d \times V_r^2 \times A \times \rho_a \times A_F$$

This static wind load does not take into account the load variation due to gust or trunk flexure. Tree height ( $h_r$ ) was taken as the distance from the base of the tree to the top of the crown. Crown height was measured from underside of crown to its top ( $C_h$ ). The crown sail area ( $A$ , m<sup>2</sup>) is that projected

toward the wind, and was assumed to remain constant for all wind speeds. Crown sail area was determined from either scaled projected photographic images or directly from field measurements and defined by height and width. The crown sail area was adjusted to reflect three parameters: the annual foliage displayed as represented by a six month factor of  $pl = 0.5$ , the parabolic shape factor  $sp = 0.67$  (Coder 2000), and a leaf plumage percentage volume fraction  $vf = 0.67$ . The leaf plumage was visually assessed as the percentage density of leaves that existed on the branches for Equation 4.

The drag coefficient ( $cd$ ) streamlining the crown was interpolated in the analytical model for the average wind velocity and up to the hurricane wind speed of 33 m s<sup>-1</sup> at the wind load application height on the crown (Equation 2). For the interpolation calculation,  $w_1$  was set to zero to represent the wind speed at calm conditions, corresponding to a  $cd$  of 0.5. The value of  $w_2$  was set to the upper limits, as referenced by Gaffrey (1999), to 20 m s<sup>-1</sup>, corresponding to a  $cd$  of 0.25. For the hurricane wind velocity of 33 m s<sup>-1</sup>, the  $cd$  was fixed at the lower published limit of 0.25. Mayhead et al. (1975) considered  $cd$  to be a constant value for wind speeds greater than 30 m s<sup>-1</sup>. For this initial study, the wind velocity ( $V_r$ , meters per second) applied at crown mid-height was given by Equation 2 (Hackel 1993) was deemed acceptable due to its simplicity. The average wind speed experienced regionally around Ladybower Dam was 4.2 m s<sup>-1</sup> (Hall 2012). The wind speed was assumed to act at 1500 mm above local ground level and converted (Equation 2) to wind speed applicable to the height corresponding to the center of the crown for the tree.

$$[2] \quad V_r = V_g \times \left( \frac{h_r}{h_g} \right)^c$$

The mathematical analysis to determine wind force retained the crown sail area as unchanging (streamlining implicit in drag coefficient) but allowed the drag coefficient to be defined by Equation 3. Because the tree's trunk profile

evolved during local average wind speeds, the average force evaluation on the crown related to local average wind speeds for the *P. sitchensis* tree.

$$[3] \quad cd = c_1 - (V - w_1) \div (w_2 - w_1) \times (c_1 - c_2)$$

The associated analytical stress (MathCad) obtained for this wind speed condition of  $4.2 \text{ m s}^{-1}$  was used to validate the FEA model only, and not used to make an assessment on the stress condition relating to fatigue life. For force evaluation on the crown of the tree at hurricane wind speeds of  $33 \text{ m s}^{-1}$ , the worst loading case that was considered was without the foliage factor applied. The three parameters stated were applied appropriately within the modification factor  $AF$  (Equation 4) that is featured in the wind force derivation (Equation 1).

The wind flow speed ( $V_r$ ) was considered as a constant for the analysis, where:

$h_r$  = Height above the ground in meters, at which wind velocity acts at crown center.

$h_g$  = The 1500 mm height above the ground in meters at which referenced wind velocity acts.

$V_g$  = Referenced wind speed at 1500 mm above the ground, measured in meters per second ( $\text{m s}^{-1}$ ).

$V_r$  = Calculated wind speed at crown center of pressure, measured in meters per second ( $\text{m s}^{-1}$ ).

$c$  = Exponent assumed for forests = 0.3.

$$[4] \quad AF = pl \times sp \times vf$$

The cross section of the trunk was assumed to remain circular (Larson 1964) and perpendicular to the y-axis (Figure 4a) while subject to the combination of tensile, shear, and compressive stresses. The greatest stress (i.e., the longitudinal tensile stress, Equation 5) was created by the wind moment effect on the outer fiber acting about one of the principal axes of the critical circular section. The sign convention is taken as positive for this longitudinal tensile stress. All stresses are assumed to remain within the elastic limits of the material.

$$[5] \quad \sigma_b = ((M_{bh} \times (D_{bh} \div 2)) \div I_{bh})$$

The center of the assumed rectangular profile of the crown leaf area (Figure 3) was taken as the position of the total acting wind force ( $F_c$ ), and its moment arm ( $hm$ ) was the distance to the critical section ( $h_g$ ) taken as 1500 mm above the local ground level. The second moment of area ( $I_{cr}$ ) is a function of the geometry of the assumed circular geometry of the section considered as circular was calculated by Equation 6.

$$[6] \quad I_{cr} = (\pi \times (D_{bh} \div 2)^4) \div 4$$

Gaffrey and Kniemeyer (2000) claimed most of the stress magnitude was due to wind-induced moments. The total bending moment calculations in this study were based only on the crown-applied wind force. The bending moment at the 1500 mm section was the product of the moment arm ( $hm$ ) and the wind force ( $F_c$ ) defined by Equation 7.

$$[7] \quad M_{cr} = F_c \times h_m$$

The weight of tree wood was obtained from published algorithms of tree weight estimates (Equation 8) (National Science Foundation 2002) and alternatively estimated from Patterson (2000). These two methods were found to agree within 5% of each other.

$$[8] \quad W_r = 0.12701 \times ((D_{bh}^2)^{1.04147}) \times ((H_g)^{0.99008})$$

The wood weight of the tree is applied over the circular cross section of trunk at the point 1500 mm above trunk base, generating a constant compressive axial stress, per Equation 9.

$$[9] \quad \sigma_d = F_D \div A_{cr}$$

Where:

$F_D$  =  $W_r$ , mass of tree (Equation 8) converted to Newtons (N).

$A_{cr}$  = Cross-sectional area of tree at critical section for this study (Equation 10).

$$[10] \quad A_{cr} = (\Pi/4) \times (D_{bh})^2$$

The wind force ( $F_c$ ) creates a drag-induced, direct shear load on the trunk that is applied

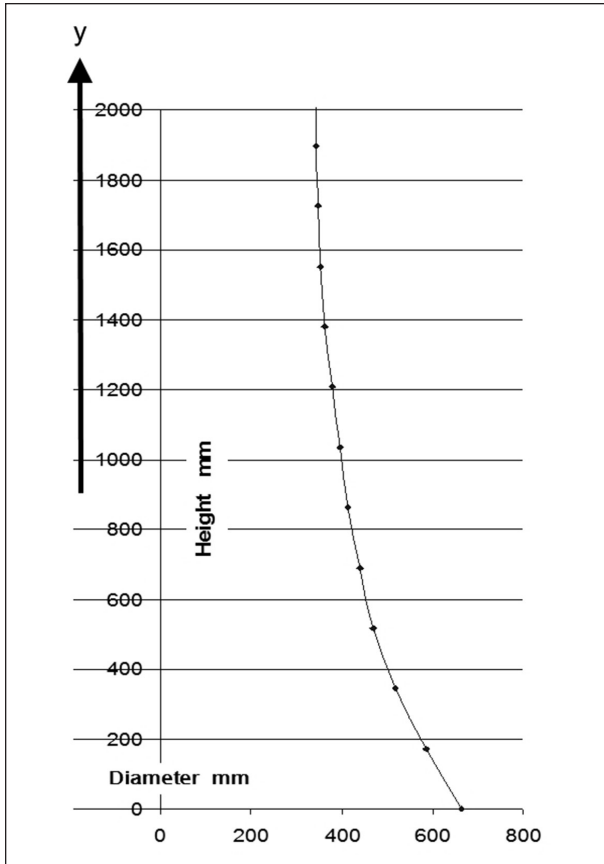


Figure 4a. Idealized tree profile.

as a uniformly distributed shear stress on the 1500 mm section. This is given by Equation 11.

$$[11] \quad fs = F_c \div A_{cr}$$

The maximum principal stress that can be compressive or tensile is the combination of the longitudinal tensile stress, the transverse shear stress due to the wind, and the stress resulting from tree self-weight. The maximum principal stress obtained from Equation 12, on the outer fiber of the trunk, was used to compare against and validate the associated finite element model's maximum principal stress results of the tree's profile under load (Roark and Young 1986).

$$[12] \quad \sigma_{mx} = (\sigma_b - \sigma_d) + fs + \sqrt{(((\sigma_b + \sigma_d) - (\sigma_d)) \div 2)^2}$$

Where:

$\sigma_b$  = Longitudinal tensile stress on the critical section due to wind bending (Equation 5).

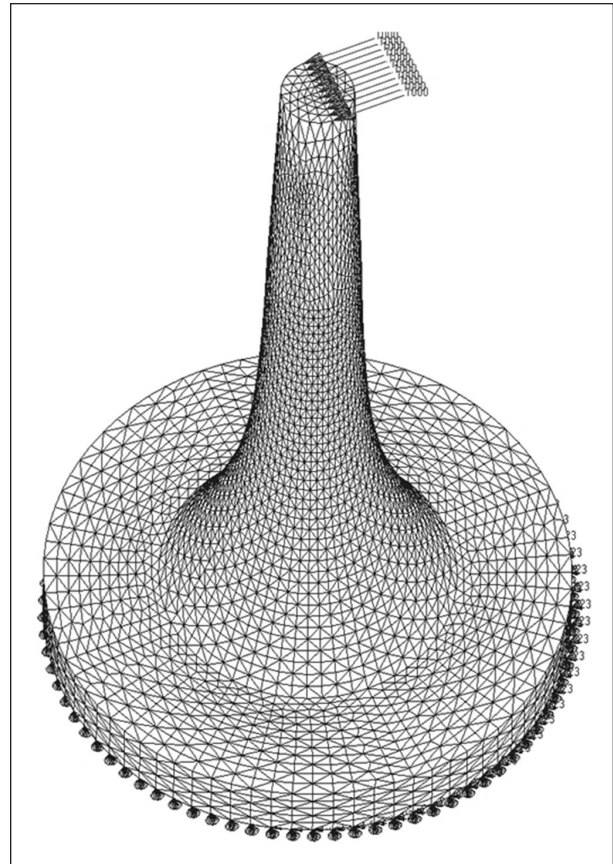


Figure 4b. FEA model fixed boundary conditions and wind load applied at tip.

$\sigma_d$  = Compressive stress due to self-weight of tree wood (Equation 9).

$f_s$  = Shear stress due to wind force (Equation 11).

The stress ratio (SR) is defined by the ratio of longitudinal tension stress (modulus) in the outer fibers of the trunk profile (Equation 5) as induced by bending related to a wind event to the compressive stress (modulus) in the trunk due to tree self-weight (Equation 13). This value is calculated and recorded for posterity.

$$[13] \quad SR = \sigma_b \div \sigma_d$$

Dimensional measurements, calculated values of tree weight, crown force, and bending moments for the *P. sitchensis* tree and its profile are listed in Table 1 and are used to construct the analytical and FEA models. The analytical stress results associated with the wind-speed loading of 4.2 m s<sup>-1</sup> are listed in

**Table 2. Calculated (in MathCad) stress results and Stress-Ratio (at 1500 mm height above ground).**

Wind velocity (m s <sup>-1</sup> )	Trunk taper	Comp. stress (N mm <sup>-2</sup> )	Shear stress (N mm <sup>-2</sup> )	Long. tensile stress (N mm <sup>-2</sup> )	Max. principal stress (N mm <sup>-2</sup> )	Stress-Ratio
4.2	-0.82	0.16	0.004	0.72	0.64	5.0

Table 2 and are in good agreement with stress levels derived in the finite element analysis of the tree profile model. This model validation supports the further intended interrogation and interpretation of the higher wind-load case FEA models considered.

### FEA MODEL DESCRIPTION

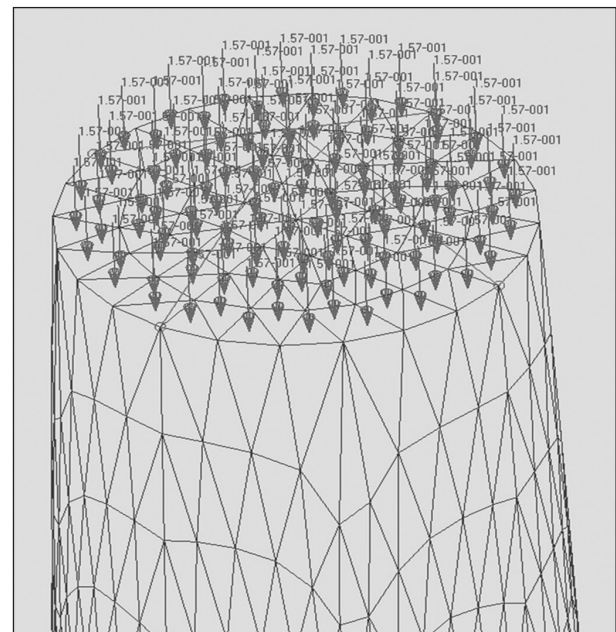
The tree profiles are theoretically devoid of stress concentrations (Uniform Stress Axiom). Therefore, the Tet4 solid elements were considered suitable for finite element analysis solid modeling of the profiles selected (Entrekin 2000).

The tree profile coordinates were orthogonally extracted from a photographic image and scaled to true size for FEA models. The profiles were constructed by selecting a smooth curve that represented the profile coordinates (Figure 4a). The curve was modelled in MSC Patran-Nastran FEA software where it was revolved about its central y-axis. A meshed surface was then produced. The MSC-Patran pre-processor offers model geometric construction capability affording a 2D-Tria4-element of approximate mesh element aspect ratio of unity to minimize error. The 2D-surface mesh was completed by sequentially extending quadrant rotations until closure was achieved at 360 degrees. A MSC-Patran instruction converted this 2D-Tria4-element surface mesh to the 3D-solid Tet4-element model of the trunk-taper consisting of 40,000 Tet4 elements and 8,000 nodes (Figure 4b). The element density is based on the preferred element aspect ratio of unity. The FEA model satisfied quality checks of node equivalencing, Jacobian ratio qualification, and element distortion. All of the profile base underside nodes degrees of freedom are fixed (Figure 4b), simulating the assumed fixity of the tree.

The load data calculated for a wind speed velocity of 4.2 m s<sup>-1</sup> produced a crown force loading of 736 N with an associated bending moment load of 1.25E+7 N mm. The respective loading for the 33 m s<sup>-1</sup> wind speed was 12,380 N and 2.11E+8 N mm. These loads were applied to consecutive but identical FE models (Table 1). A published mean value of Young's Modulus of 7,900 N mm<sup>-2</sup> for *P. sitchensis* was assumed

throughout the FE model. The combined load of bending (due to wind forces) and compression (from tree self-weight) is applied to the FEA model as follows: the bending load is applied as a unidirectional point force attached to each node along the diameter line on the top surface of the model (Figure 4b).

The self-weight of the tree was converted to a pressure uniformly distributed over the cross section of the stem. However, in growing structures such as trees, it is accepted that this pressure is higher in older wood rings. As a consequence, the young wood in the outer regions is not load bearing or even submitted to tensile stresses resulting from longitudinal maturation strains of newly differentiated cells (Fournier et al. 2006). The area extent of this young wood was unknown in the study and the compressive load was applied to the top surface of the top elements (Figure 5). This presents an acceptable variation of less than 1.0% of the maximum principal stress at the hurricane wind speed. This maximum variation in the stress level can be reached, for instance, in broadleaf trees forming tension wood that can generate tensile stresses of about 10 MPa near the cambium (Fourcaud et al. 2003).

**Figure 5. Tree self-weight applied as a pressure load.**

## RESULTS

### FEA Investigation of *P. sitchensis* in Snake Pass, Derbyshire

Inherent in the simplicity of the method of load attachment at single node entities (Figure 6a; Figure 6b; Figure 7a; Figure 7b), stress singularities are generated as depicted by the localized red (topmost dark) zone at the top of the FEA models. The stress hot spot is an artifact of the limitations of the method of load implementation on finite element models Sinclair (2012). The convention is to accept stresses that have stabilized remote from the affected region, and for this model assessment a position of 87.5% above tree profile base was chosen.

The combined effects of local average wind speed of  $4.2 \text{ m s}^{-1}$  with tree self-weight are examined in the FEA model analysis shown in Figure 6a. The full 34 m of *P. Sitchensis* tree profile was not modeled due to practical restrictions. However, for this study, the region of interest of stress results and distribution was from the profile base to the underside of the tree crown. From the total 5600 mm profile analyzed, up to 3000 mm (53%) from profile base exhibited a surface maximum principal stress of under  $0.7 \text{ N mm}^{-2}$ . The profile stress was low level and its stress distribution was non-uniform. The maximum stress range appearing at the upper realms of the profile was an order of magnitude greater than the stress at the base of the profile. Stress distribution in the FEA models representing the  $24.5 \text{ m s}^{-1}$  (Figure 6b) and  $33 \text{ m s}^{-1}$  (Figure 7a; Figure 7b) load cases was also non-uniform. A plotted graph of the surface profile maximum principal stress to the profile height (Figure 6a; Figure 6b) for the average wind speed of  $4.2 \text{ m s}^{-1}$  and for the hurricane wind speed of  $33 \text{ m s}^{-1}$  load case, respectively, are given in Figure 8. The FEA model stress analysis for the  $35 \text{ m s}^{-1}$  is shown in Figure 7b.

The results of the stress analysis for various wind speeds are tabulated in Table 3. The list includes

the maximum principal stress at the surface of the profile at a height of 1500 mm above local ground level, the associated stress components of longitudinal tensile stress, self-weight compressive stress and Stress-Ratio. The magnitude of the FEA stress results were validated by the similarity to the analytical MathCad model values. This provided confidence of the stress values along various profile heights.

### HURRICANE-INDUCED LOW CYCLE FATIGUE FAILURE

Close to the surface of the tree profile is the longitudinal cambium, most of which is directionally aligned with the axis of the trunk. Crack initiation begins at the tree's surface, as this is the position of highest stress due to its greater distance from the tree's neutral axis. The calculations show for the hurricane wind speed of  $33 \text{ m s}^{-1}$  that the shear stress component (Equation 11) in the surface due to the wind force is negligible at 0.5% of the maximum principal stress (Table 2). In this case, the corresponding angle of the maximum principal stress defines its principal direction as the normal stress acting as tension or compression on the wood grain. The maximum principal stress is compared to the allowable wood rupture stress for the static strength calculation and for fatigue life derivation.

A series of wind-load cases from the average wind speed up to and exceeding the hurricane wind-speed load case were made to the *P. sitchensis* profile FEA model. The position of maximum principal stress is assumed at 87.5% of profile height. This is a position considered sufficiently remote from the influence of the point of load application (singularity) in the tree profile of the non-uniform stress distribution in the profile surface. The corresponding results are tabulated in Table 4. The maximum applied stress on the surface profile of the *P. sitchensis* for the hurricane wind speed of  $33 \text{ m s}^{-1}$  was assessed at  $23 \text{ N mm}^{-2}$  (Figure 7a; Figure 7b) and corresponded to 72% of the ultimate wood breaking strength of

**Table 3. Calculated stress results and Stress-Ratio (at 1500 mm height above ground) for *Picea sitchensis*.**

Wind velocity ( $\text{m s}^{-1}$ )	Long. tensile stress ( $\text{N mm}^{-2}$ )	Shear stress ( $\text{N mm}^{-2}$ )	Comp. stress ( $\text{N mm}^{-2}$ )	Max. principal stress ( $\text{N mm}^{-2}$ )	Stress-Ratio
4.2	0.72	0.004	0.16	0.64	5
24.5	2.68	0.013	0.16	2.61	
33.0	6.27	0.032	0.16	6.21	40
35.0	7.07	0.036	0.16	7.01	

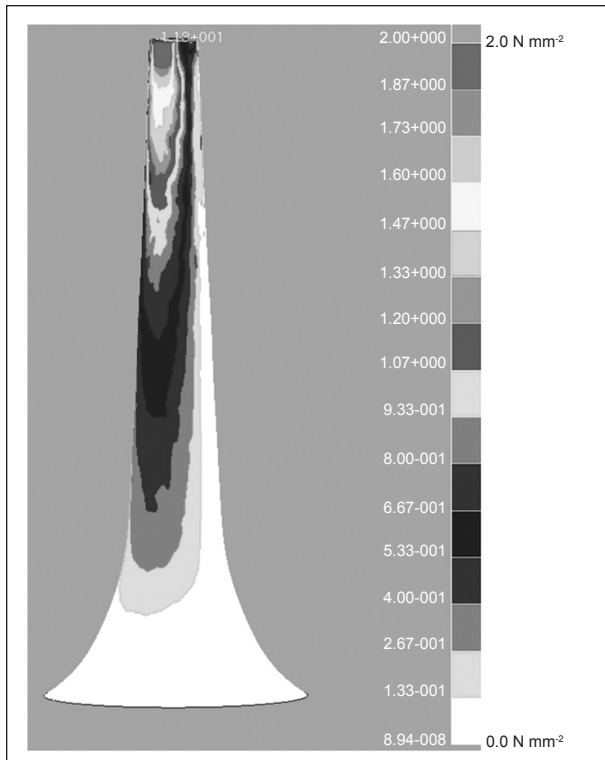


Figure 6a. Stress response related to self-weight and average wind speed of 4.2 m s<sup>-1</sup>. Max. principal stress. (Max. stress scale 2 N mm<sup>-2</sup>).

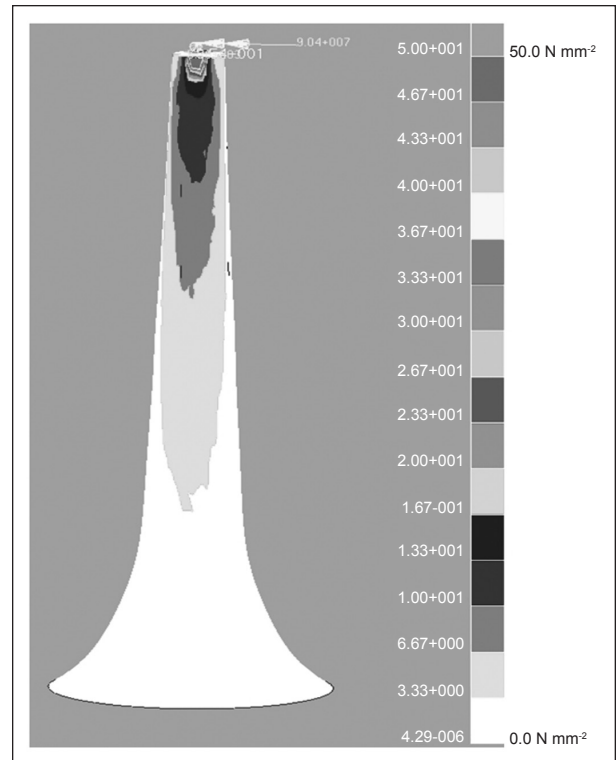


Figure 6b. Stress response related to self-weight and average wind speed of 24.5 m s<sup>-1</sup>. Max. principal stress (Max. stress scale 50 N mm<sup>-2</sup>).

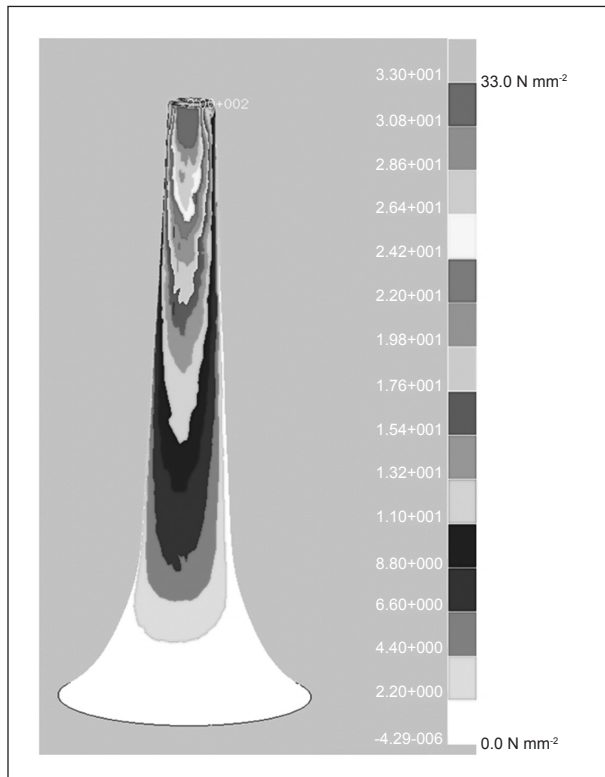


Figure 7a. Stress response related to self-weight and hurricane wind speed 33 m s<sup>-1</sup>. Max. principal stress. (Max. stress scale 33 N mm<sup>-2</sup>).

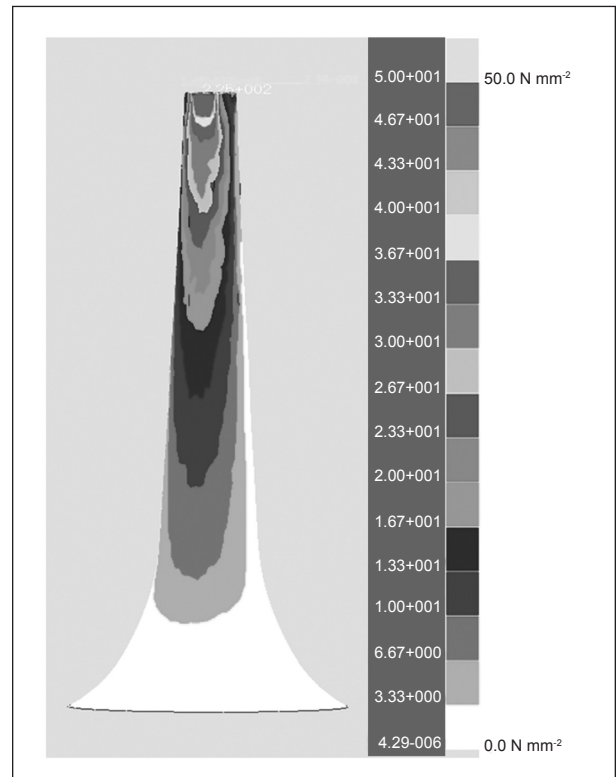


Figure 7b. Stress response related to self-weight and hurricane wind speed 35 m s<sup>-1</sup>. Max. principal stress. (Max. stress scale 50 N mm<sup>-2</sup>).

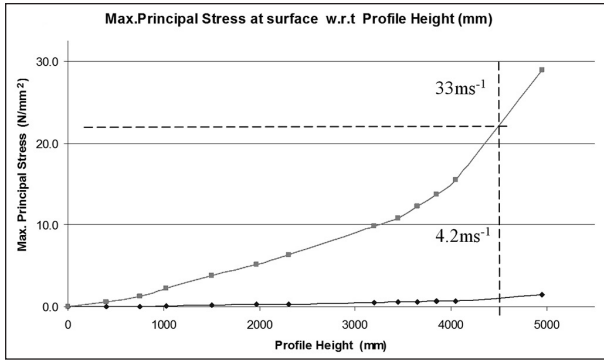


Figure 8. Maximum principal stress at profile’s surface for the load case of local average wind speed of 4.2 m s<sup>-1</sup> and hurricane wind speed of 33 m s<sup>-1</sup>.

32 N mm<sup>-2</sup>. This stress status, when expressed as a conventional static strength reserve factor, gives a value of 1.4 comparable to the bending moment reserve factor of 1.51 that James et al. (2006) published. The maximum principal stress in the surface profile of *P. sitchensis* correspondingly increased with wind speed from 24.5 m s<sup>-1</sup> to 35 m s<sup>-1</sup> and is shown as a power relationship in Figure 9. Wind gust as a dynamic and periodic event exposing the tree to trunk sway produces the greatest load, and if transient structural demands surpass the materials static strength, then trunk breakage will result (James et al. 2006). Fatigue failures usually occur at regions of geometrical discontinuity or other areas of high stress concentration. A general definition of a stress concentration is provided in Equation 14.

$$[14] \quad k_t = \text{Maximum localised elasticstress} \div \text{averageStress}$$

The analysis has shown that the tree profile did not develop a stress concentration, but evidence of high stress in the profile stress distribution was located in the upper regions of the profile as previously stated. Low cycle fatigue calculations utilized the maximum principal surface stress results of the tree profile. This was structured with data from two sources of reviewed literature; Bao and Gibson (1996); for stress-related fatigue life cycles (S-N curve data) assumed applicable for *P. sitchensis* species (Tsai and Ansell 1990) and sway frequency, Coder (2000) revealed cycles and time to failure of the trunk under different, sustained wind-speed loadings (Table 4). Cycles to failure for each load case stress was obtained from the reproduction of the S-N fatigue life scatter-plot of percentage stress level

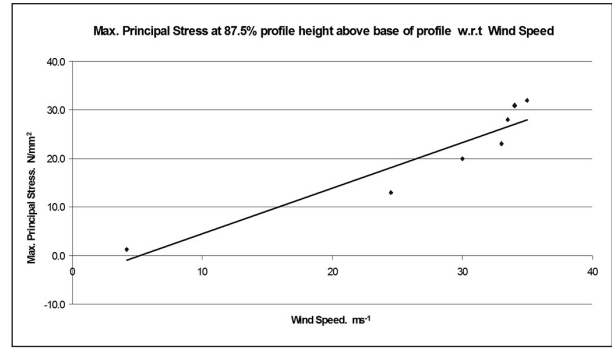


Figure 9. Maximum principal stress in *Picea Sitchensis* profile surface at 87.5% of profile height.

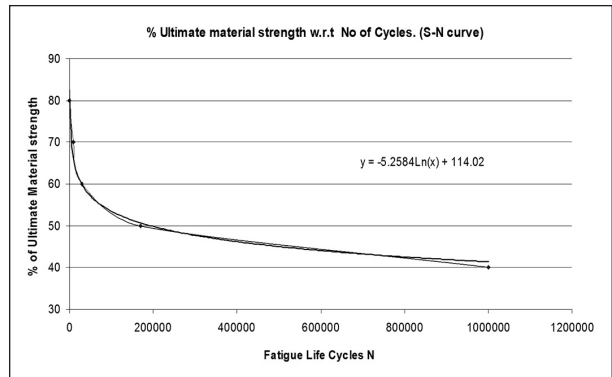


Figure 10. Percent stress level versus fatigue life cycles (Bao and Gibson 1996).

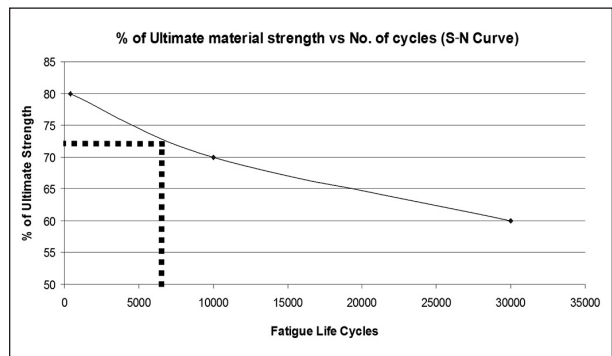


Figure 11. A localized range of the graph shown in Figure 10.

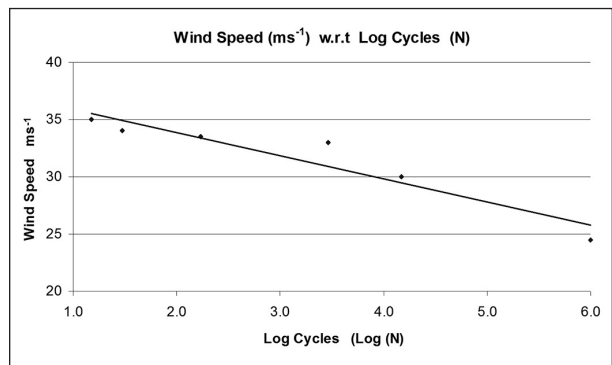


Figure 12. Wind speed m s<sup>-1</sup> to log cycles fatigue failure (N).

**Table 4. Wind speeds, % of  $F_{tu}$  stress level (at 87.5% profile height) w.r.t predicted fatigue life cycles and hours to failure for the *Picea Sitchensis* tree.**

Wind velocity (m s <sup>-1</sup> )	% of material $F_{tu}$	Max. principal stress (N mm <sup>-2</sup> )	% above ground stress measured on FEA model	No. of cycles to fatigue failure (N)	Time to failure (minutes)	Time to failure (hours)	Log cycles [log (N)]	Log time (minutes)
24.5	41	13	87.5	1000000	52632	877.20	6.00	4.72
30.0	63	20	87.5	15000	789	13.20	4.18	2.90
33.0	72	23	87.5	2900	153	2.60	3.46	2.18
33.5	88	28	87.5	170	9	0.15	2.23	0.95
34.0	97	31	87.5	30	2	0.03	1.48	0.20
35.0	100	32	87.5	15	0.8	0.00	1.18	-0.10

of ultimate wood strength versus fatigue life cycles (Figure 2), from Bao and Gibson (1996), for wood samples. Percentage stress of ultimate material strength ( $F_{tu}$ ) is given by Equation 15.

$$[15] \quad \%F_{tu} = (\sigma \div F_{tu}) \times 100$$

### Fatigue Cycles to Failure

The corresponding fatigue strength given by the number of cycles to failure of the stem for the hurricane wind speed of 33 m s<sup>-1</sup> is obtained from the maximum principal surface stress on the profile located at 4,800 mm above profile base (87.5% profile height) and was 23 N mm<sup>-2</sup> (Figure 8). This value corresponds to 72% of the ultimate strength of *P. sitchensis* wood (Table 4). By iteration of Equation 16, which defines the S-N fatigue life-cycle curve the LCF failure of trunk, is derived at 2,900 cycles (Figure 10).

$$[16] \quad y = -5.2584 \times \ln(X) + 114.02$$

The quality of the graph (Figure 10) extracted from the original presented by Bao and Gibson (1996) is of low fidelity. This is discernable by a comparison of the equation-derived value (Equation 16) to the LCF value, obtained graphically as 7,400 cycles (Figure 11).

Log cycles to fatigue failure of the trunk versus a wind-speed range from 24.5 m s<sup>-1</sup> to 35 m s<sup>-1</sup> is given in Figure 12.

### Fatigue Time to Failure

The height of the tree in this survey was 34 m, which corresponds to a tree sway frequency of 19 cycles per minute (Coder 2000). Dividing the number of cycles to failure by the frequency resulted in the

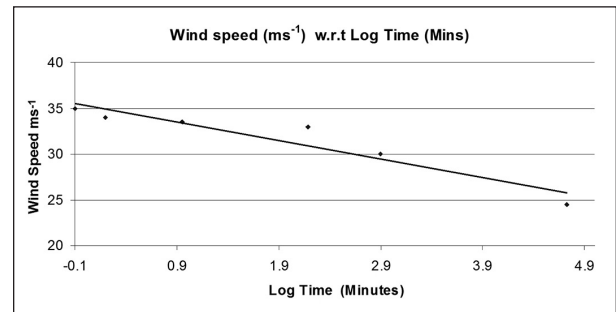


**Figure 13. Wind speed m s<sup>-1</sup> to log time fatigue failure in minutes.**

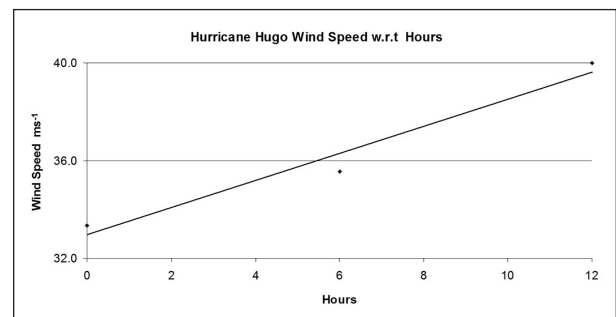


**Figure 14. Data for Hurricane Hugo, 1989. Wind speed m s<sup>-1</sup> increase against hours.**

fatigue time to failure of the trunk in minutes or hours relative to the particular sustained wind speed. The results of the fatigue calculations on the tree profile are given in Table 4, which lists the corresponding number of cycles to fatigue failure and the corresponding time in minutes and hours to failure for the different wind speeds examined. The calculation for this study was based on full periodic reversal loading.

By the stated method, the calculated time to fatigue failure of the *P. sitchensis* trunk under a sustained hurricane wind speed of 33 m s<sup>-1</sup> was 2 hours and 38 minutes (2.6 hours).

Figure 13 provides a graphical relationship for log time to fatigue failure of the trunk versus a wind-speed range from 24.5 m s<sup>-1</sup> to 35 m s<sup>-1</sup>.

### Hurricane Wind Duration

A number of sources report sustained wind speeds of Hurricane Hugo (September 21–22, 1989), of the Carolina's area of the eastern United States, were 33 m s<sup>-1</sup> on average for two hours, and gusting to above 35 m s<sup>-1</sup> for two hours (Powell et al. 1991;) (Figure 14).

## DISCUSSION

Low surface stress values of 0.34 N mm<sup>-2</sup> at breast height were reported by Morgan and Cannell (1993) from their mathematical pine tree profile model exposed to a local average wind speed of 5.0 m s<sup>-1</sup>; this was assumed as an approximate uniform stress distribution. However, the findings of the current report of the mathematical *P. sitchensis* profile FEA model, developed for the local average wind speed loading of 4.2 m s<sup>-1</sup> produced a similar low stress of 0.65 N mm<sup>-2</sup> when compared to the wood's ultimate strength of 34 N mm<sup>-2</sup>. But this investigation revealed a non-linear distribution of stress magnitude, increasing with height from profile base, existing for average wind up to and exceeding hurricane force wind loads on the *P. sitchensis* surface profile. The stress levels in the upper reaches of the profile were generally an order of magnitude greater than the stress at the base of the profile. Insufficient data in the literature was found to show if a profile adapts to ensure the probability of failure is not equal but biased in favor of an elevated profile failure to increase the prospect of the plant's survival.

The endurance limit appears to occur a little below the wind speed of 24.2 m s<sup>-1</sup>, which corresponds to stress levels at 0.41 of the wood's rupture strength, allowing 105 cycles to failure. A surface stress level of 23 N mm<sup>-2</sup> was calculated at the 87.5% of profile height of the *P. sitchensis* profile FEA simulation predicting a fatigue life failure within 2.6 hours of cyclic exposure to the hurricane wind force of 33 m s<sup>-1</sup>. The corresponding failure cycles were established from an equation that referenced a graphical extraction of the original graph by Bao and Gibson (1996). Graphical examination in the low cycle region depicted in Figure 11 provides the number of cycles to failure as 7,400. The associated

failure time would then be 6.5 hours. This stress level corresponds to 72% of the ultimate strength of *P. sitchensis* and supports the observation by Kane et al. (2000) that stem failures due to excessive stress were observed at positions on tree trunks where the applied stress was 79% of the ultimate material strength. At a slightly higher wind speed of 35 m s<sup>-1</sup> the calculated trunk fracture occurred after only 15 cycles, equivalent to 48 seconds. Additionally, widespread stem breakage of 81% of a Scots pine (*Pinus sylvestris* L.) population was reported by the tree model simulations of hurricane events made by Holland et al. (2006).

Stem failure is a dynamic event. Emphasizing the relationship of these hurricane wind-speed occurrences in the literature and observational data strengthens the notion that failure of the *P. sitchensis* stem was by LCF.

## CONCLUSION

A method was developed in this investigation of low cycle fatigue life analysis and applied to a *Picea sitchensis* tree profile exposed to various wind loads up to and exceeding hurricane wind speeds of 33 m s<sup>-1</sup>. Results of the analysis are summarized.

1. The *P. sitchensis* tree profile was found to have a non-uniform maximum principal stress distribution. The maximum stress range appeared at the upper realms of the profile, in general, at an order of magnitude greater than the stress at the base of the profile.

2. The static analysis for the hurricane wind speed of 33 m s<sup>-1</sup> indicated an adequate material strength in the trunk represented as a strength reserve factor of 1.4. This suggested a different mode of failure.

3. The predicted duration of the trunk fatigue fracture event of 2 hours and 38 minutes was in general agreement with the average passage time of Hurricane Hugo wind speed of 33 m s<sup>-1</sup> (Figure 14).

4. The hypothesis that LCF had an influence on the failure scenario of trunk breakage is consistent with associated literature and witness data.

The methodology developed attempted to provide a predictive model for the *P. sitchensis* tree's susceptibility to LCF damage induced by hurricane winds. Although this model was indicative, the accuracy may be improved by statistical data

obtained by analyzing many *P. sitchensis* tree profiles. An improved definition of the original S-N curve data by Bao and Gibson (1996) would significantly enhance accuracy of the LCF model. Further understanding and model predictive accuracy may be improved by the application of the appropriate load-spectra stress-cycle history data of the tree profile to the Palmgren and Miner Cumulative damage rule, which incorporates fatigue damage caused by various stress cycles and magnitudes.

**Acknowledgments.** The author would like to thank Tania Leigh, Ph.D., for her advice on certain aspects of the contents to this paper and to Jayme Leigh who helped with the tree survey and the construction of the finite element models.

### LITERATURE CITED

- Bao, Z., C. Eckelmann, and H. Gibson. 1996. Fatigue strength and allowable design stresses for some wood composites used in furniture. *Holz als Roh- und Werkstoff* 54:377–382.
- Clorius, O.C. 2002. An investigation in tension perpendicular to the grain. Technical University of Denmark. 176 pp.
- Coder, K. 2000. Sway frequency in tree stems. School of Forestry Resources, The University of Georgia, United States of America.
- Cullen, S. 2005. A practical consideration of the drag equation velocity exponent for urban tree risk management. *Journal of Arboriculture* 31(3):101–113.
- Cullen, S. 2002. Trees and wind: Wind scales and speeds. *Journal of Arboriculture* 28(5):237–242
- Entrekin, A. 2000. Accuracy of MSC/Nastran First and Second order Tetrahedral Elements in Solid Modelling for Stress Analysis. Bell Helicopter. Texas, United States of America.
- Farmers Forest. 2006. Tree and Forest measurement journal. United States of America
- Fons, L., and Pong, W.Y. 1957. Tree breakage characteristics under static loading-ponderosa pine. USDA. Forest Service Interim Tech Report. United States of America.
- Fourcaud, T., F. Blaise, P. Lac, P. Castera, and P. de Reffye. 2003. Numerical Modelling of Shape Regulation and Growth Stresses in Trees II. Implementation in the AMAPpara software and simulation of tree growth. *Trees, Structure, and Function* 17:31–39.
- Fournier, M., A. Stokes, C. Coutand, T. Fourcaud, and B. Moulia. 2006. Tree Biomechanics and Growth Strategies in the Context of Forest Functional Ecology. pp. 1–33. In: A. Herrel, T. Speck, and N. Rowe (Eds.). *Ecology and Biomechanics: A Mechanical Approach to the Ecology of Animals and Plants*. CRC Press Taylor & Francis, Boca Raton, Florida, U.S.
- Francis, J., and A. Gillespie. 1993. Relating gust speed to tree damage in Hurricane Hugo, 1989. *Journal of Arboriculture* 19(6):368–373.
- Gaffrey, D., and O. Kniemeyer. 2002. The elasto-mechanical behavior of Douglas-fir, its sensitivity to tree-specific properties, wind and snow loads and implications for stability—a simulation study. Faculty of Forest Sciences and Forest Ecology. Institute of Biometry and Informatics. Gottingen, University of Gottingen. Germany.
- Gaffrey, D. 1999. Simulated Stress Distribution in a Stem of a 64 year old Douglas fir. Applying a 3D: Tree Load Model. Institute of Forest Biometry, University of Gottingen, Germany.
- Gong, M., and I. Smith. 2000. Failure mechanism of softwood under low cycle fatigue load in compression parallel to grain. Faculty of Forestry. University of New Brunswick, Canada. 8 pp.
- Hackel, H. 1993. *Meteorologie*. Ulmer Verlag, Stuttgart, Germany.
- Hall, B. 2012. British Meteorological Office. <www.metoffice.gov.uk>
- Holland, A., and A. Riordan, and E. Franklin. 2006. A simple model for simulating tornado damage in forests. *Journal of Applied Meteorological Climatology* 45:1597–1611
- James, K., N. Haritos, and K. Ades. 2006. Mechanical stability of trees under dynamic loads. *American Journal of Botany* 93(10):1522–1530.
- James, K., and N. Haritos. 2006. Dynamic wind loads on trees. School of Resource Management, University of Melbourne, Australia.
- Kane, B., R. Farrell, S.M. Zedaker, J.R. Loferski, and D.W. Smith. 2008. Failure Mode and Prediction of the Strength of Branch Attachments. *Arboriculture & Urban Forestry* 34(5):308–316.
- Larson, R.P. 1964. Stem Form of Young Larix as Influenced by Wind and Pruning. By Lakes States Forest. United States of America.
- Leigh, W. 2012. A Strength-Index of tree species susceptibility to hurricane wind damage (unpublished). Cranfield University. Cranfield, Bedfordshire, Great Britain.
- Mattheck, C. 1991. *Trees: The Mechanical design*. Springer-Verlag, Berlin, Germany.
- Mayhead, G.J., J.B. Gardiner, and D.W. Durrant. 1975. A report on the physical properties of conifers in relation to plantation stability. R&D Division. British Forestry Commission. Unpublished report.
- Moore, J. 2011. Wood properties and uses of Sitka spruce in Britain. Forestry Commission, Edinburgh. Great Britain.
- Morgan, J., and M. Cannell. 1993. Shape of tree stems—a re-examination of the uniform stress hypothesis. *Tree Physiology* 14:49–62.
- National Science Foundation. 2002. *Tree weight Algorithms*. Shodor Education Foundation Inc., United States of America.
- Niklas, K., and F. Molina-Freaner. 1999. Wood Biomechanics and anatomy of *Pachycereus pringlei*. Department of Plant Biology, Cornell University, United States of America.
- Patterson, D. 2000. Landowner's guide to determining weight of standing hardwood trees. Division of Agriculture, University of Arkansas. United States of America.
- Petty, J.A., and C. Swain. 1985. Factors influencing stem breakage of conifers in high winds. Department of Forestry, University of Aberdeen. Great Britain.
- Powell, M.D., P.P. Dodge, and M.L. Black. 1991. The landfall of the Hurricane Hugo in the Carolinas: Surface wind distribution. Hurricane Research Division, Florida. United States of America. *Weather Forecast* 6:379–399.
- Ratnasingam, J., and F. Ioras. 2010. Static and fatigue strength of oil palm wood used in furniture. *Journal of Applied Sciences* 10:986–990.
- Roark, J., and W. Young. 1986. *Formulas for Stress and Strain*, fifth edition. McGraw-Hill, New York City, New York, U.S.
- Tsai, K., and M. Ansell. 1990. The Fatigue properties of wood in flexure. *Journal of material science* 25:865–878.

Wilson, B., and R. Archer. 1979. Tree Design: Some Biological Solutions to Mechanical Problems. Department of Forestry and Wildlife Management, The University of Massachusetts, United States of America.

Warren B. Leigh, Ph.D.  
School of Engineering  
Cranfield University  
Cranfield, Bedfordshire MK43 0AL, UK  
jurajet@yahoo.com

**Zusammenfassung.** Kiefernplantagen sind wegen der hohen zyklischen Stresslevel in Verbindung mit starken Winden sehr anfällig für Stammbruch. Die Stressanalyse und die Modelle mit begrenzter Element-Simulation wurden auf ein repräsentatives Profil von Sitka-Fichten konstruiert. Der Profil-Oberflächen-Stress (S) wurde bestimmt durch eine kombinierte Last aus Baumeigengewicht und Sturmwindgeschwindigkeit. Die Ergebnisse wurden ergänzt durch die Referenz zweier anderer Studien durch andere Forscher, die den Einfluss von Ermüdungsphasen auf das Versagen von Kiefernholz (N) untersuchten und Baumschwingzyklen zur Vorhersage von Stammversagen. Die Position des maximalen Profil-Oberflächen-Stress und die Stelle des beginnenden Stammbruchs wurden bestätigt durch eine nicht-uniforme Stress-Antwort. Bei keiner untersuchten Windlast wurde eine Stress-Uniformität entlang des Stammprofils beobachtet. Das analytische Modell und die Analyse der begrenzenden Elemente des Sitka-Fichten-Stammprofils enthüllten einen statistisch adäquaten Kraftreservfaktor von 1,4, was bedeutet, dass andere Versagenskräfte verantwortlich waren. Die Vorhersage von Lebensermüdung wurde unter zyklischen und Stressamplituden in Verbindung zu Windgeschwindigkeiten von 33 m s<sup>-1</sup> untersucht. Eine vorhersehbare Stammfraktur trat innerhalb von 2,6 h auf, welche sich dramatisch reduzierten auf 2 min bei einer Zunahme der Windgeschwindigkeit auf 1 m s<sup>-1</sup>.

Die kalkulierte Zeit der Exposition war vergleichbar mit der aufgezeichneten Zeit während des Sturms Hugo in 1989. Die Vorhersage der Zeit bis zum Versagen, die durch die Analyse-Methoden dieser Studie ermittelt wurde, schien plausibel und das damit verbundene Profil der Sitka-Fichten bei niedrigen Ermüdungszyklen Stammbruch erleiden würde.

**Resumen.** Las plantaciones de pino son propensas a la rotura de los tallos debido a los altos niveles de estrés cíclicos asociados con la fuerza de los vientos de los huracanes. Se construyeron modelos de simulación por elementos finitos y análisis de estrés en un perfil representativo de un árbol de *Picea sitchensis* (Sitka). El perfil de estrés superficial (S) se determinó con base a la carga combinada del peso propio árbol y la velocidad del viento del huracán. Los resultados se complementaron con referencia a otros dos estudios realizados por otros investigadores que estudiaron el impacto de los ciclos de fatiga a la falla (N) de la madera de pino y los ciclos de balanceo de árbol para presentar una predicción de la fatiga del tallo. Se determinó la posición de la tensión máxima superficial y la iniciación de la falla del tronco a partir de una respuesta de estrés no uniforme. No se observó una tensión uniforme a lo largo del perfil de tronco para cualquier carga examinada. El modelo analítico y el análisis de elementos finitos del perfil del *P. sitchensis* revelaron un factor de reserva de fuerza estática adecuada de 1,4, lo que sugiere que otro modo de fracaso era el responsable. La predicción de falla se examinó bajo amplitud cíclica y del mismo estrés relacionado con la velocidad del viento del huracán de 33 m s<sup>-1</sup>. La fractura del tronco predicho se produjo en 2,6 horas, lo que se redujo dramáticamente a dos minutos con un aumento en la velocidad del viento

de sólo 1 m s<sup>-1</sup>. El tiempo de exposición calculado fue similar al registrado durante el huracán Hugo en 1989. La predicción del tiempo de falla obtenido por el método de análisis lo hizo parecer posible y el perfil asociado con *P. sitchensis* podría sufrir rotura del tallo por ciclo de fatiga (LCF).